Application of Magnetic Pulse Welding for Aluminum Alloys and SPCC Steel Sheet Joints

Welding process parameters and characteristics were developed for a variety of similar and dissimilar metals magnetic pulse welds

BY T. AIZAWA, M. KASHANI, AND K. OKAGAWA

ABSTRACT. Magnetic pulse welding (MPW) is a cold process for welding conductive metals to similar or dissimilar materials. Magnetic pulse welding uses magnetic pressure to drive the primary metal against the target metal sweeping away surface contaminants while forcing intimate metal-to-metal contact, thereby producing a solid-state weld. In this paper, the MPW method and its application for several aluminum alloys (A1050, A2017, A3004, A5182, A5052, A6016, and A7075) and joints in steel (SPCC) sheets were investigated, and the welding process parameters and characteristics are reported.

Introduction

One of the most difficult problems in welding is to weld dissimilar metals such as aluminum and steel together. Hybrid structures of aluminum alloy and steel are suggested for reducing the weight of automobiles to improve fuel efficiency and control air pollution. Therefore, the joining of steel and aluminum alloy in different shapes is receiving attention. However, steel and aluminum are not compatible metals as far as fusion welding is concerned. The reason for this is attributed to the large difference between their melting points (660°C for Al and 1497°C for steel), the nearly zero solid solubility of iron in aluminum, and the formation of brittle intermetallic compounds such as Fe_2Al_5 and $FeAl_3$. Further, differences in their thermal properties such as expansion coefficients, conductivities, and specific heats lead to internal stresses after fusion welding. Therefore, fusion welds of steel and aluminum suffer from heavy cracking with brittle failure in service. The material properties of aluminum and steel are summarized in Table 1.

Magnetic pulse welding (MPW) provides an excellent tool for achieving aluminum to steel sheet joints. Magnetic pulse welding is a solid-state joining process of conductive metals. The welding process is heat-free, which can eliminate localized annealing. This paper describes MPW formation in the dissimilar joining of aluminum alloys (A1050, A2017, A3004, A5182, A5052, A6016, and A7075) and steel plate cold rolled commercial grade (SPCC).

A typical MPW system includes a power supply, which contains a bank of capacitors, a fast switching system, and a coil. The parts to be joined are inserted into the coil, the capacitor bank is charged, and the low inductance switch is triggered by a pulse trigger system and the current flows through the coil. When current is applied to the coil, a high-density magnetic flux is created around the coil, and as a result an eddy current is created in the workpieces. The eddy currents oppose the magnetic field in the coil and a repulsive force is created. This force can drive the workpieces together at an extremely high rate of speed and creates an explosive or impact type of weld. For more conductive metals, such as aluminum and copper, less energy is required to achieve a weld. The conventional MPW method with solenoidal coil is used for joining tubular parts and its features are most well known (Refs. 1–3). However, a few papers on MPW of sheet workpieces have been reported.

In a previous paper, we proposed a new one-turn flat coil instead of the solenoidal coil. This coil consisted of upper and lower H-shaped plates, which we call the double layer H-shaped coil. The overlapped sheet workpieces were inserted between these two H-shaped plates. When the high current flows through the coil, it can create the magnetic field to both sides of the overlapped sheet workpieces, and as a result, the sheet metals were welded in the seam state. The magnetic flux produced by this type of coil is shown in Fig. 1A. In this method, the eddy currents that flow in both sheets are considerably different when dissimilar sheet metals like Al/steel sheets are welded. And, also, the thickness of the workpieces was limited by the space between two H-shaped plates. Therefore, for more applications, some contrivance or improvement was needed. These experimental results and welding characteristics for several samples such as Al-Al (Ref. 4), Al-Cu (Ref. 5), Al-Mg, Al-Ti, and Al-Fe (Ref. 6) were reported in previous papers.

In the present experiment, a new coil was designed to improve the welding characteristics of Al alloy and SPCC-steel sheet joints. This new coil is a one-layer E-shaped flat coil that the overlapped sheet workpieces were put on the one side of the coil (Fig. 1B). This type of coil can be designed for applications ranging from short and small to large and long workpieces and also T-shaped joints with higher weld quality.

KEYWORDS

Magnetic Pulse Welding
Seam Welding
Dissimilar Metal
Aluminum Alloys
Steel

Experimental Procedures

MPW Principle

The principle of the magnetic pulse welding method for one Al/Fe sheet sample is shown in Fig. 2. When a high current is applied to the coil, a high magnetic flux density **B** is suddenly generated and penetrates into Al/Fe sheets, then the eddy currents (current density **i**) pass through them to hinder its further penetration. As a result, an electromagnetic force of $\mathbf{i} \times \mathbf{B}$ acts mainly on the Al sheet and the Al sheet is accelerated away from the coil and collides rapidly with the steel sheet. At the

*TOMOKATSU AIZAWA and MEHRDAD KASHANI (*kashani@asrl.org*) are with Department of Electronic and Information Engineering, and KEIGO OKAGAWA is with Department of Electrical Engineering, Tokyo Metropolitan College of Technology, Shinagawa-Ku, Tokyo, Japan.*

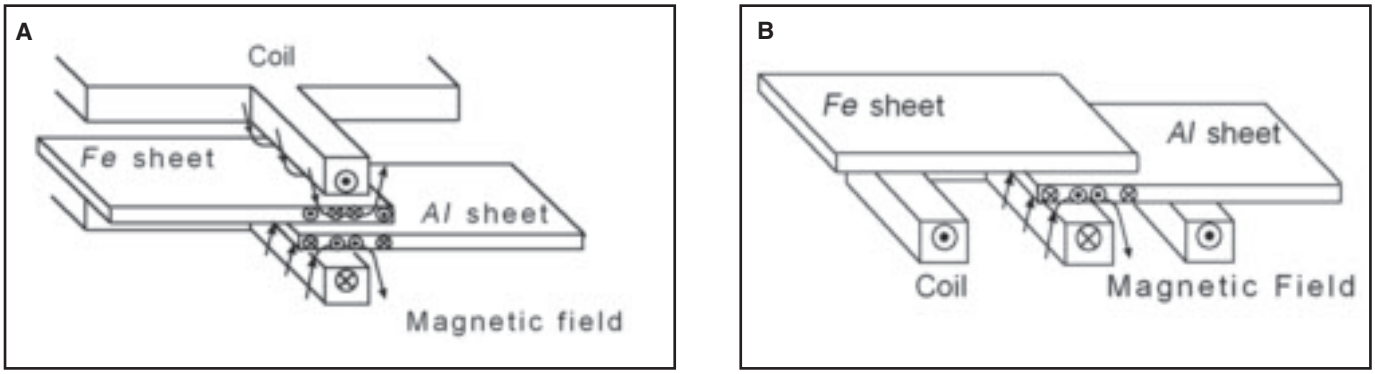

Fig. 1 — MPW coil structure. A — Double-layer, H-shaped flat coil; B — one-layer E-shaped flat coil.

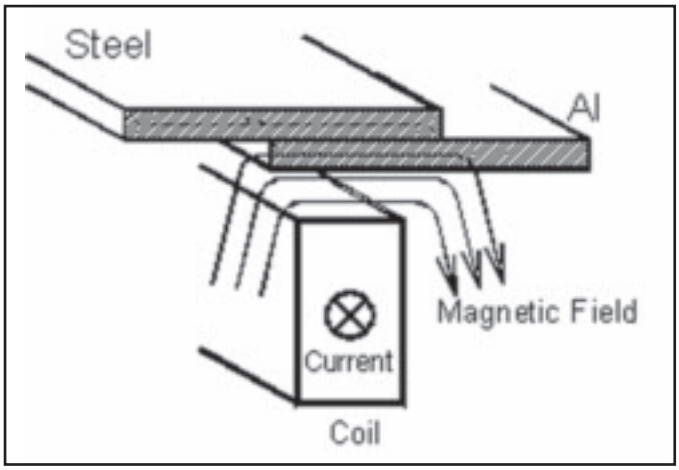

Fig. 2 — Principle of MPW for welding of the Al/steel sheet sample (cross-section view).

moment of collision, the colliding surfaces can be cleared by a large kinetic energy getting before the collision. After the collision, the cleared surfaces are being pressed together by electromagnetic force and a fixture.

The eddy current i and the magnetic pressure p are given as follows:

$$\nabla \times \boldsymbol{i} = -\kappa\left(\frac{\partial \boldsymbol{B}}{\partial t}\right) \qquad (1)$$

$$p = \left(B_o^2 - B_i^2\right)/2\mu = \left(\frac{B_o^2}{2\mu}\right)\left(1 - e^{-2x/\delta}\right)$$

$$\text{and } \delta = \sqrt{2/\omega\kappa\mu} \qquad (2)$$

where κ, μ, τ, B_o, and B_i are the electrical conductivity, magnetic permeability, thickness, and magnetic flux density at lower and upper surfaces of Al sheet, respectively. The depth of skin effect can be obtained by $\delta = \sqrt{2/\omega\kappa\mu}$, where ω is the angular frequency of changing field.

When the eddy current flows through the workpieces, Al sheet is pressed to the Fe sheet by magnetic pressure and is heated by a Joule heating effect ($Q = i^2/\kappa$). Equation 1 shows that more eddy currents are produced at the surface of the metal sheet for materials that have a higher electrical conductivity κ and, as a result, the stronger magnetic pressure p and a large amount of Joule heat are generated during the weld process. In addition, from Equation 2 it can be obtained that the magnetic pressure also increases for higher conductive materials.

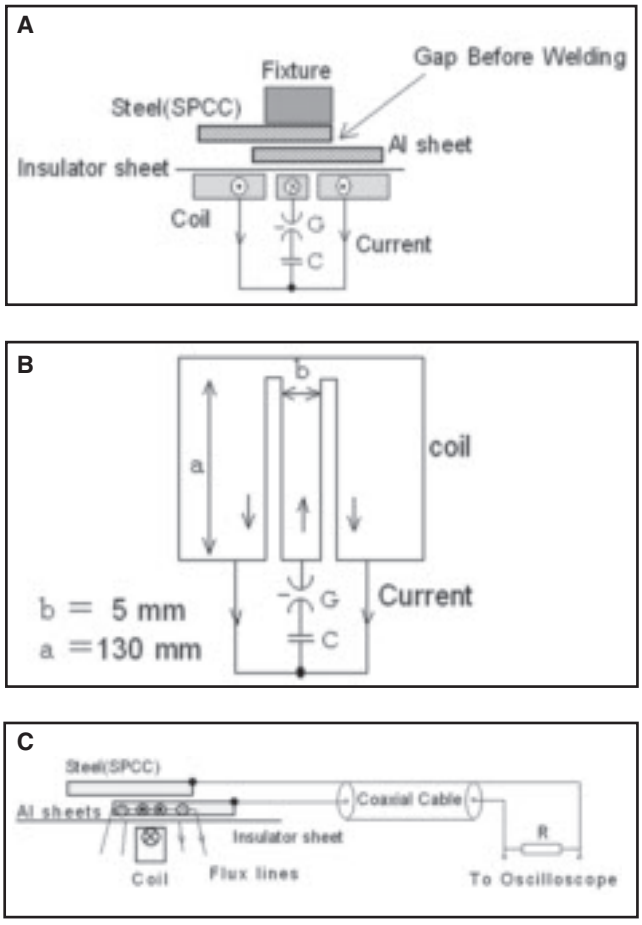

Fig. 3 — General outlines of apparatus. A — Cross-section view of the coil containing lap of Al/steel (SPCC) sheets and discharge circuit; B — plan view of coil with discharge circuit; C — collision speed measurement. C denotes the capacitor bank and G the gap switch.

Table 1 — Aluminum and Steel Properties

	Melting Point °C	Specific Heat J/kg.°C	Density kg/m^3	Thermal Conductivity J/m^3.°C.s	Electrical Resistivity μΩ.cm
Aluminum	660	900	2700	220	2.65
Steel	1497	460	7870	73	13.30
Al/Steel Ratio	0.44	1.96	0.34	0.33	0.20

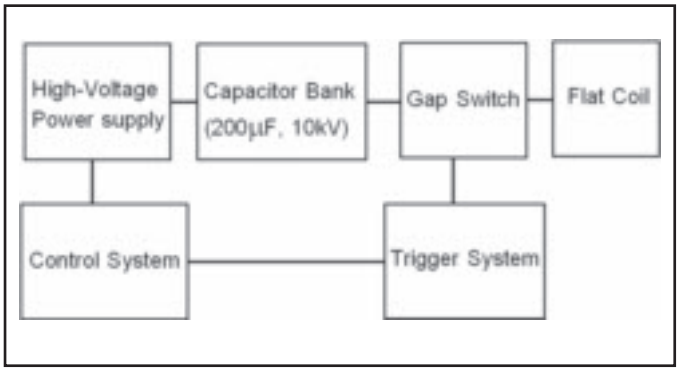

Fig. 4 — The block diagram of the discharge system.

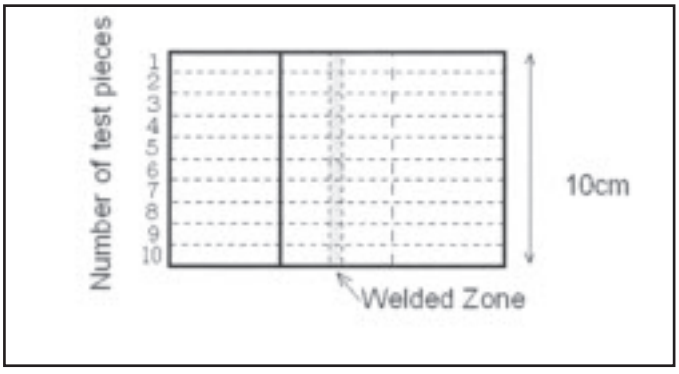

Fig. 5 — Divided region of the welded sample for shearing tensile test, optical micrograph, and SEM image observations.

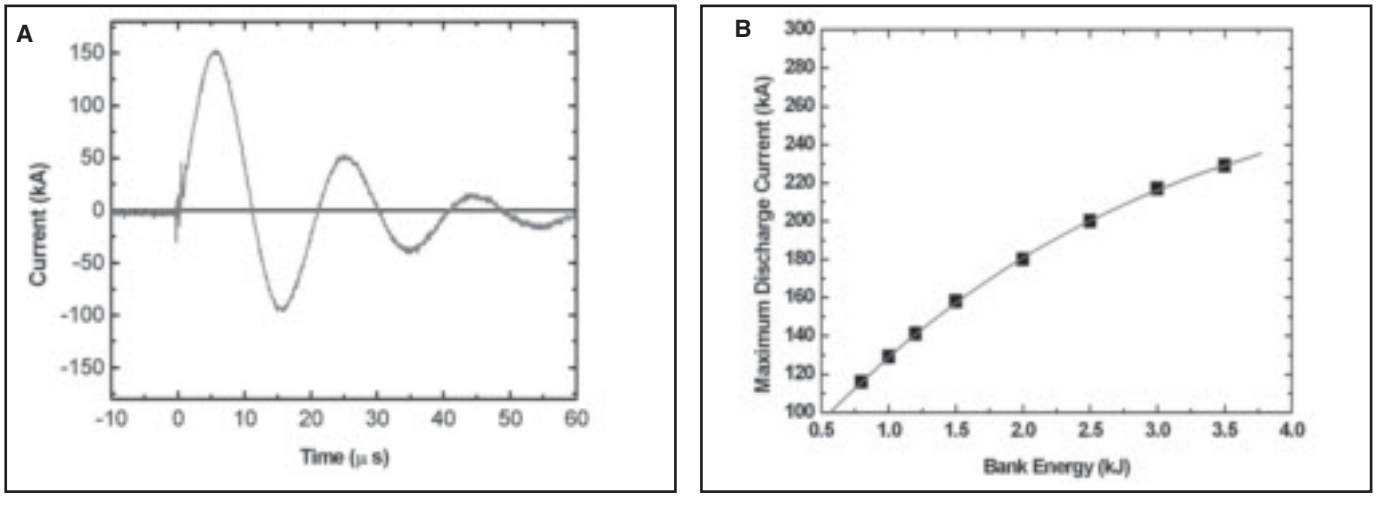

Fig. 6 — A — Typical current signal at 1.4-kJ discharge (200 μF/3.8 kV); B — bank energy vs. maximum discharge current.

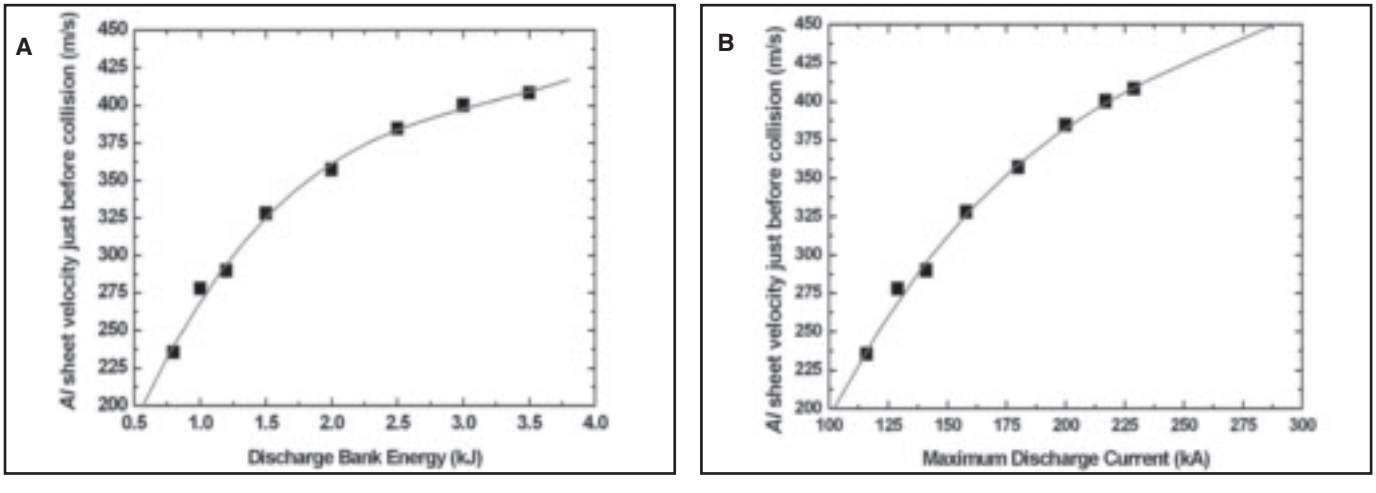

Fig. 7 — The speed of the Al sheet just before collision vs. the following: A — Discharge bank energy; B — maximum discharge current.

Experimental Apparatus

Figure 3 shows the general outlines of the magnetic pulse welding apparatus, which consists of a capacitor bank (C) and a spark gap switch (G) with a one-layer, E-shaped flat coil. It was attempted to make a low-inductance discharge circuit that can generate a high-density magnetic flux around the coil area.

The capacitor bank that drives the discharge system of the MPW device consists of two capacitors of 100 μF/10 kV in parallel. The inductance of the bank capacitor is 0.02 μH, and it is connected to the gap switch and one-turn coil by a low-inductance transmission line. The circuit is designed to keep the inductance as low as possible to carry out fast welding. The flat, E-shaped, one-turn coil was made of a Cr-Cu alloy. The coil thickness is 2 mm and the inductance of the coil is 0.04 μH. The block diagram of the discharge system is shown in Fig. 4. When the gap switch is

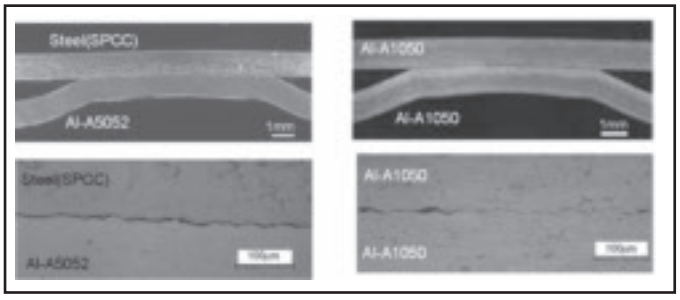

Fig. 8 — Typical microstructure of joined interface zone for A1050/A1050 and A5052/SPCC.

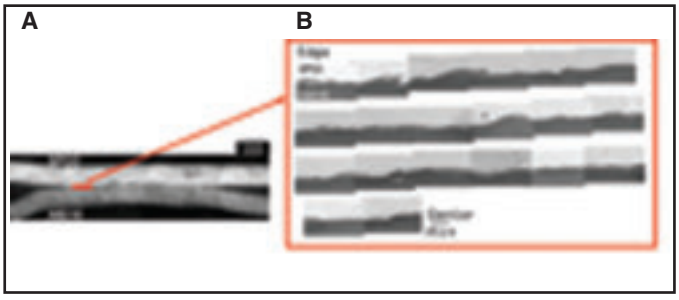

Fig. 9 — A — Cross-section image of welded sample (the red zone is the observation area by SEM); B — SEM image of joined interface for A6016/SPCC sample.

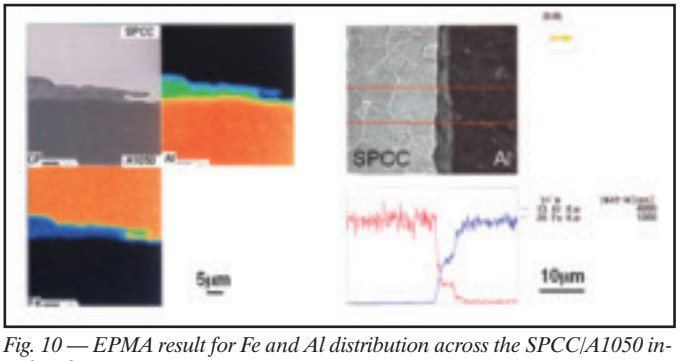

Fig. 10 — EPMA result for Fe and Al distribution across the SPCC/A1050 interface layer.

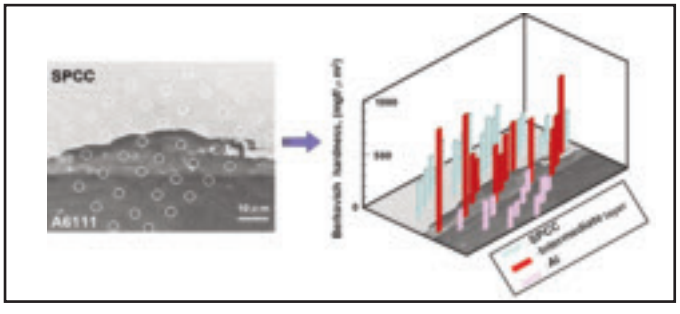

Fig. 12 — Typical microstructure of the interface layer of the A6111/SPCC sample, including Berkovich hardness indentation across the interface.

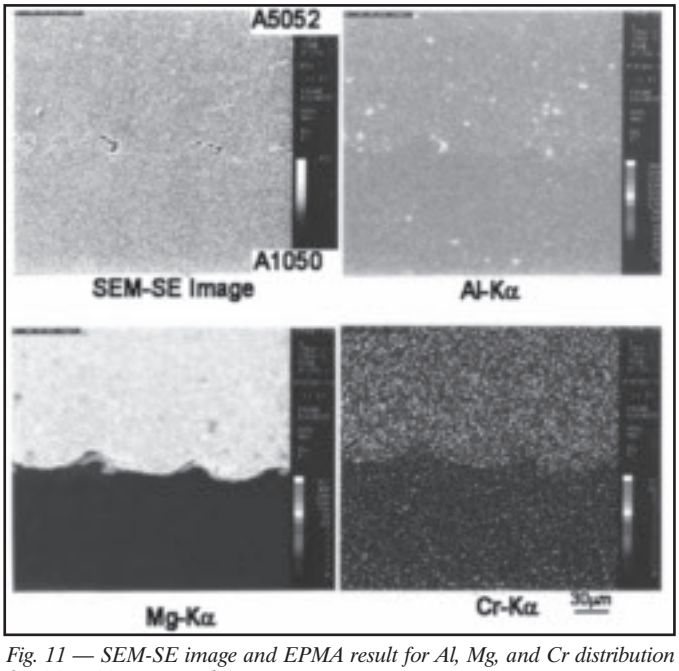

Fig. 11 — SEM-SE image and EPMA result for Al, Mg, and Cr distribution for A1050/A5052 sample.

Table 2 — The Aluminum Alloy and SPCC Steel Characteristics

Sample Specification	A1050	A2017	A3004	A5182	A5052	A6016	A7075	SPCC
Conductivity [IACS•]	61	49	41	33	35	53	45	13
Tensile Strength [MPa]	165	187	255	360	290	212	292	350

closed, an impulse discharge current from the capacitor bank (C) passes through the coil and the MPW process begins.

Aluminum alloy (A1050, A2017, A3004, A5182, A5052, A6016, and A7075) and steel (SPCC) sheets were prepared to carry out the weld process. The characteristic parameters of the aluminum alloys and SPCC steel that were used in the experiments are shown in Table 2.

The size of all samples was 100 mm long and 100 mm wide with a thickness of 1.0 mm. The contact surface between two samples was polished and cleaned with abrasives and methanol. The 0.1~0.3-mm-thick insulating sheets were loaded between the coil surface and the overlapped ends of the workpiece sheet. It was ascertained that the welding characteristics could be improved by fixing the initial root opening (0.5~1 mm) between two metal sheets. The optimization of root opening distance is described in the section titiled "collision speed measurement."

It should be noted here that the more conductive metal works as a base metal (Al sheet is the base metal for the Al/SPCC workpieces), and the main eddy current appears in the base metal. The coil is clamped with the fixture during the welding operation. After welding, the welded sample was divided into ten pieces for tensile shearing strength tests and optical micrograph and scanning electron microscope (SEM) image observations — Fig. 5.

Experimental Results and Discussion

Discharge Current and Flux Density

A typical current waveform is shown in

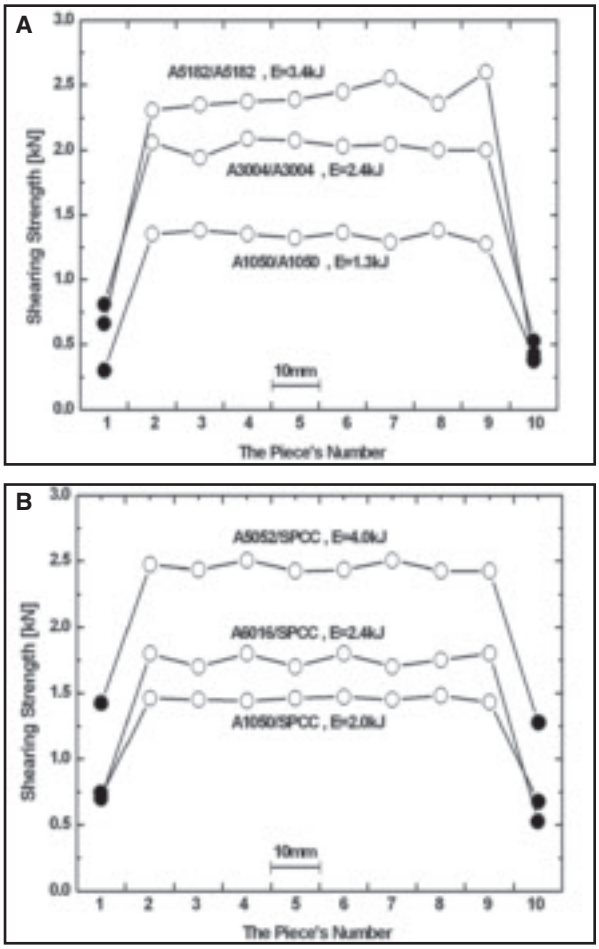

Fig. 13 — Distribution of tensile shear strength for ten divided pieces of the welded samples. A — A1050/A1050, A3004/A3004, and A5182/A5182 sheets; B — A1050/SPCC, A5052/SPCC, and A6016/SPCC sheets: ❍ The rupture of base metal, ● the rupture of the welded area.

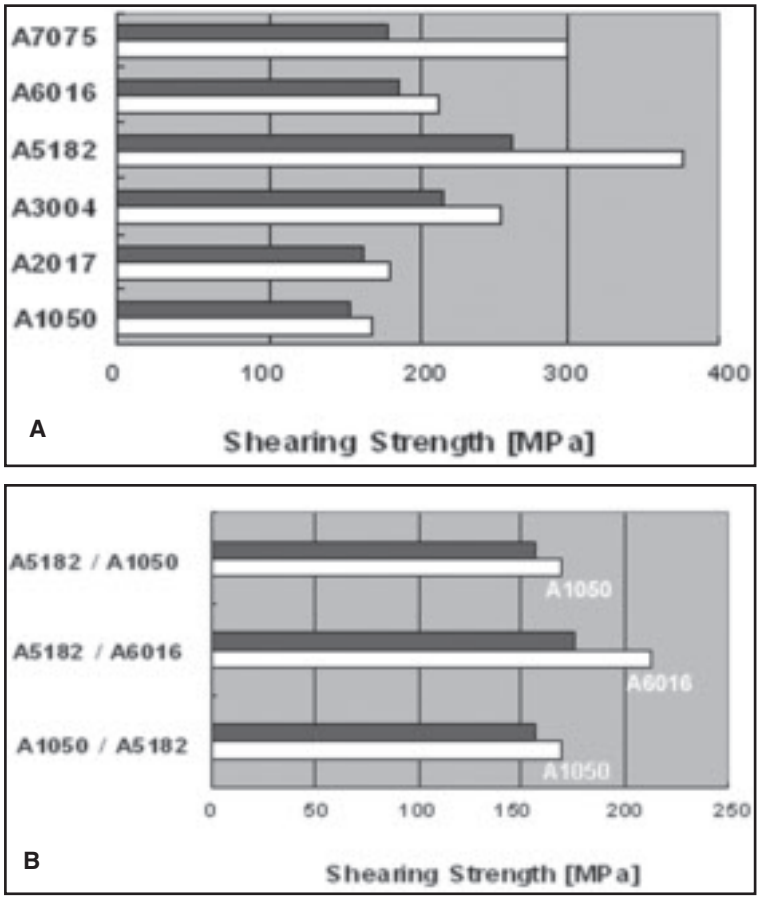

Fig. 15 — Comparison of the maximum tensile shear strength for the following: A — The same aluminum alloy combinations; B — different aluminum alloy combinations: ■ The maximum tensile shearing strength of welded sample. ❑ The maximum tensile shearing strength of the base alloy without weld.

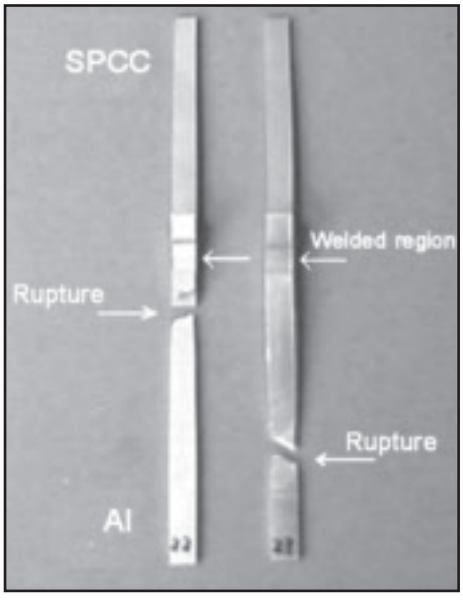

Fig. 14 — Typical rupture of Al alloy in the tensile shear strength test of SPCC/Al joints.

Fig. 6A. This current signal was obtained at 1.4-kJ discharge (200 μF/3.8 kV) by using a magnetic probe. The current signal shows that a damping and oscillating current flows through a one-turn coil for the duration of about 50 μs and the oscillating period is about 22 μs. The maximum current was measured at about 150 kA at 1.4 kJ bank energy discharge. The relation between the bank energy and discharge current in our system is shown in Fig. 6B.

If the discharge current flows uniformly on the surfaces of the middle portions of the coil, then the depth of skin effect ($\delta=\sqrt{2/\omega\kappa\mu}$) was calculated at 0.38 mm for Al sheet, and under this condition, the maximum magnetic flux density is estimated at about 20T, while the maximum magnetic pressure is calculated at about 150 MPa from Equation 2.

Collision Speed Measurement

In order to measure the collision speed of the aluminum sheet just before welding, a simple circuit was prepared to measure the time of travel of the base metal in the root opening that existed between the two workpieces before welding. The circuit consists of a coaxial cable and matching resistance — Fig. 3C (Ref. 7).

When the impulse discharge current passes through the coil, a voltage is induced on the two workpieces by magnetic coupling between the coil and these workpieces. Just after the collision, the voltage appears at input terminals of the measuring circuit and that voltage signal can be detected by a digital oscilloscope. If we assume that the sheet movement is like a uniform acceleration motion, the collision speed just before welding can be estimated by using the time of travel and root opening distance. The collision speed has a relation with the bank energy and the discharge current and the maximum collision speed can be obtained at the first maximum in the current signal. Therefore, by inserting the appropriate root opening between sample sheets, the collision time can be nearly the same as quarter period of the current signal at the first maximum current peak. The optimum root

opening has a relation with the capacitor bank energy and the discharge system inductance. However, our experimental result shows that a 0.5~1 mm root opening between sheets is necessary for achieving high weld quality in the aluminum alloy and steel sheet joint. Figure 7 shows the Al sheet speed just before collision vs. the maximum current and bank energy.

Microstructure of Joined Interface

The width of the weld zone was nearly equal to the middle part of the coil (b = 5 mm). The welded sheets were divided into ten 10-mm-wide test pieces as shown in Fig. 5, and one longitudinal side of the division of No. 5 was polished for observing the joined interface. Several welded combinations of Axxxx/Axxxx and Axxxx/ SPCC steels were tested. For the similar workpieces, the joined interface was not very clear. However, in the aluminum alloy and SPCC steel combination after etching and polishing, the interface layer were clearly seen against the base metals. Typical macrostructure of the joined interface zone for A1050/A1050 and A5052/SPCC are shown in Fig. 8. As a result of magnetic pulse welding, a nonuniform wavy interface is visible for all welded samples. The wavy interface zones were formed with amplitudes as high as 20 μm and widths of 100 μm. Figure 9 also shows the macrostructure of the joined interface zone for an A6016/SPCC combination.

The SEM image of A6016/SPCC also shows that the wavy morphology weld-interface was formed in the interface layer without any significant heat-affected zone (HAZ).

Electron Probe Microanalysis (EPMA)

The result of an EPMA test for SPCC/A1050 combination is illustrated in Fig. 10. A single step decrease was observed in the EPMA profile for all combinations (Al/SPCC) across the interface. The EPMA result shows that the 5-μm-wide transition layer is formed in the welding interface.

Figure 11 shows the secondary electron images obtained by scanning electron microscopy (SEM-SE) and also EPMA of Al, Mg, and Cr in the A1050/A5052 interface layer. The EPMA result for Mg clearly shows that a wavy bond interface was formed in the welded zone.

Microhardness Profile

To obtain the nano-hardness profile of the interface layer, the Berkovich indenter was used. Figure 12 shows the interface microstructure along with traces of the Berkovich nano-hardness indentations for the A6111/SPCC sample. The hardness measurement across the interface layer clearly shows that the hardness of the intermediate layer is higher than the aluminum base metal in all points. The reason for this higher hardness at the intermediate results from intense plastic deformation due to a high-velocity collision or to a fine-grain microstructure that was formed by rapid solidification of the welded interface.

Tensile Shear Test

Welded samples were investigated on a standard tensile shear testing machine at a test rate of 10 mm/min. Tensile shear tests were made for each ten divided pieces to determine the maximum shear tensile strength. The test results for Al/SPCC and aluminum alloy combination are shown in Fig. 13, where a mark (❍) indicates the rupture of based metal and (●) a rupture of the welded area. Based on the shear strength test results, the tensile shear of divisions No. 1 and No. 10 were less than the others. However, in other divisions the failures always occurred in the weaker metal and outside of the welded area. Figure 14 shows the typical rupture of based metal for SPCC/Al joints.

The comparison of the maximum tensile shear strength for the same aluminum alloy combinations and different aluminum alloy combinations are shown in Fig. 15. The results of division No. 5 in Fig. 5 was used for this consideration.

The comparison of the maximum tensile shear for the same alloy combination (Fig. 15A) shows that except for A5182/A5182 and A7075/A7075 joints, the maximum tensile shearing for all other cases is nearly the same as the tensile shear strength of base metal without a weld and for different alloy combinations (Fig. 15B), the maximum tensile shear strength of the welded sample is also the same as a weaker base metal value. It can be pointed out that the sheet metals retain their original properties without the heat-affected zone problems during the weld process, and the welded zone is stronger than the weaker base metals so failure always occurred outside of the welded zone for these combinations. These results would be expected for a solid-state joining process.

Conclusions

We can determine the solid-state weld quality achievable for most aluminum alloys and SPCC steel combinations using the MPW method. Our experimental results show that the weld joint is always stronger than the weaker metal and in all tested combination a discontinuous or continuous pocket-type, wavy transition layer was formed without any significant heat-affected zone. The capability of our MPW method has also been successfully examined for several other types of metal joints, such as T-joints, circular joints, and long sheet samples (up to 500 mm).

Acknowledgments

The authors wish to express thanks to Professor K. Ikeuchi of Osaka University and Dr. M. Kumagai of Sumitomo Light Metal Industries Ltd. for fruitful and useful discussions. The authors also would like to thank Professor S. Kumai of Tokyo Institute of Technology for the observation of the joined interface and Mr. M. Matsuda of Chuo Seisakusho Ltd. for useful help about the EPMA test.

References

1. Brower, D. F. 1969. *Metals Handbook* 4 Forming. Metals Park, Ohio: ASM International, p. 256.

2. Shribman, V., Stern, A., Livshitz, Y., and Gafri, O. 2002. Magnetic pulse welding produces high-strength aluminum welds. *Welding Journal* 81(4): 33.

3. Masumoto, I., Tamaki, K., and Kojima, M. 1980. *Journal of the Japan Welding Society* 1(49): 29.

4. Aizawa, T., Okagawa, K., Yoshizawa, M., and Henmi, N. 2001. *Proc. of 4th Int. Symposium on Impact Engineering*, Kumamoto, Japan, p. 827.

5. Aizawa, T., and Yoshizawa, M. 2001. *Proc. of 7th Int. Symposium of Japan Welding Society*, Kobe, Japan, p. 295.

6. Aizawa, T., and Kashani, M. 2004. *Proc. of IIW International Conference on Technical Trends and Future Prospective of Welding Technology for Transportation, Land, Sea, Air and Space*, Osaka, Japan.

7. Okagawa, K., and Aizawa, T. 2004. *Proc. of International Conference on New Frontiers of Process Science and Engineering in Advanced Material*, Kyoto, Japan, p. 501.